Cubic Metric Reduction by Hybrid Companding-Universal Filtered Multi-carrier in 5G Networks

Farooq Sijal Shawqi [1, *], Lukman Audah [1], Sameer Alani [2], Ahmed Talaat Hammoodi [3], and Mohammed Ahmed Jubair [4]

[1] Faculty of Electrical and Electronic Engineering, Universiti Tun HusseinOnn Malaysia 86400 Parit Raja, BatuPahat, Johor, Malaysia; Email: hanif@uthm.edu.my (L.A.)
[2] Computer Center, University of Anbar, Iraq; Email: sameer.h@uoanbar.edu.iq (S.A.)
[3] Head of the Control Systems and Communications Department AlAnbar University, Iraq; Email: ahmed.talaat@uoanbar.edu.iq (A.T.H.)
[4] College of Information Technology, Imam Ja'afar Al-Sadiq University, Al-Muthanna 66002, Iraq.
*Correspondence: farooquthm@gmail.com (F.S.S.)

***Abstract*—There are several different waveforms used by the latest generation of wireless communication technologies. The Universal Filtered Multicarrier (UFMC) was selected because of its compatibility with a wide variety of numerology systems and its symmetrical nature. However, the high peak-to-average power ratio (PAPR) is a significant challenge for UFMC designs. While the Power-Averaged Perceived Roughness (PAPR) metric pinpoints the signal's highest point, the Cubic Metric (CM) pinpoints its out-of-band (OoB) and in-band (IB) distortion. Scrambling techniques like Selection Mapping (SLM) increase BER efficiency, while A-law and -law companding has been advanced to cut down on out-of-band interference (OBI) and PAPR, respectively. For companding techniques that don't introduce any distortions to the signal but increase PAPR and system complexity, the composite approach is utilized. Through simulation in MATLAB, we find that the SLM-companding UFMC model provides superior CM performance. For high-order modulation (256QAM), the CCDF-CM was reduced to 52% relative to eight-phase rotation vectors, a significant improvement over the standard UFMC.**

***Keywords*—cubic metric reduction, 5G networks, universal filtered multicarrier**

I. Introduction

New wireless communication technology has been expanding with larger data rates, which naturally leads to bigger bandwidths with low latency and good Quality of Service (QoS) [1, 2]. This is all due to the increasing popularity of online games and other multimedia services. According to [3], it is expected that 5G technology would have a greater data rate, system capacity by more than a factor of 1000 cell throughput by more than a factor of 25, and spectral efficiency by more than a factor of 10. Different topologies, modulation symbol formats, and/or sizes are required by the evolving waveform network communications standards [4, 5]. Frequency division multiplexing (FDM), orthogonal frequency division multiplexing (OFDM), and state-of-the-art cyclic prefix-orthogonal frequency division multiplexing (CP-OFDM) are all examples. As a part of 4G's Long-Term Evolution (LTE), CP-OFDM has seen widespread commercial deployment. But CP-OFDM fell short in LTE due to the need to accommodate a variety of numerologies and communication circumstances. Other forms of multiplexing include Filter Bank Multicarrier (FBMC), filtered Orthogonal Frequency Division Multiplexing (f-OFDM) [6, 7], and Universal Filtered Multicarrier (UFMC), also known as universal filtered OFDM (UF-OFDM) [8]. It is widely agreed that the UFMC is the optimal waveform for 5G networks [9–11].

The time-domain coherence of subcarriers is the primary cause of the high Peak-to-Average Power Ratio (PAPR) that plagues multicarrier modulation schemes [12]. The fundamental problem with the CP-OFDM system is the high PAPR, which has a detrimental effect on bit error rate (BER) performance and causes spectral corruption. High-performance HPAs are the standard method for avoiding the PAPR issue [13]. However, they are often costly and bulky. Besides, operating the HPA in the linear zone requires a considerable input back-off power, which reduces the efficiency of the power amplifier and increases the system's overall power consumption. Another approach that has been offered to battle the PAPR value is to increase the average power of the signal. However, this solution decreases the signal-to-noise ratio, which in turn degrades the BER performance [14, 15]. Therefore, decreasing the peak strength of the CP-OFDM signal before transmission is the proper answer to the high PAPR value. Many methods for reducing PAPR have been proposed in the literature to address this issue (see Fig. 1), and these methods may be roughly divided into two groups: one group introduces distortion, and the second group does

Manuscript received April 27, 2023; revised June 5, 2023, accepted June 9, 2023.

not introduce distortion [16, 17]. The former enhances signal characteristics in the frequency domain or time domain to lessen PAPR before transmission, while the latter destroys the high peak of the CP-OFDM signal in the time domain before transferring.

The signal to the HPA. At the price of in-band distortion and out-of-band radiation, signal-distortion methods may drastically lower the PAPR value [18, 19]. As a result, the OFDM system's BER performance and frequency spectrum will degrade in ways that are not acceptable [20, 21]. Clipping the signal, clipping and filtering, peak windowing, and companding transformations are all examples of methods that distort the signal [22–25].

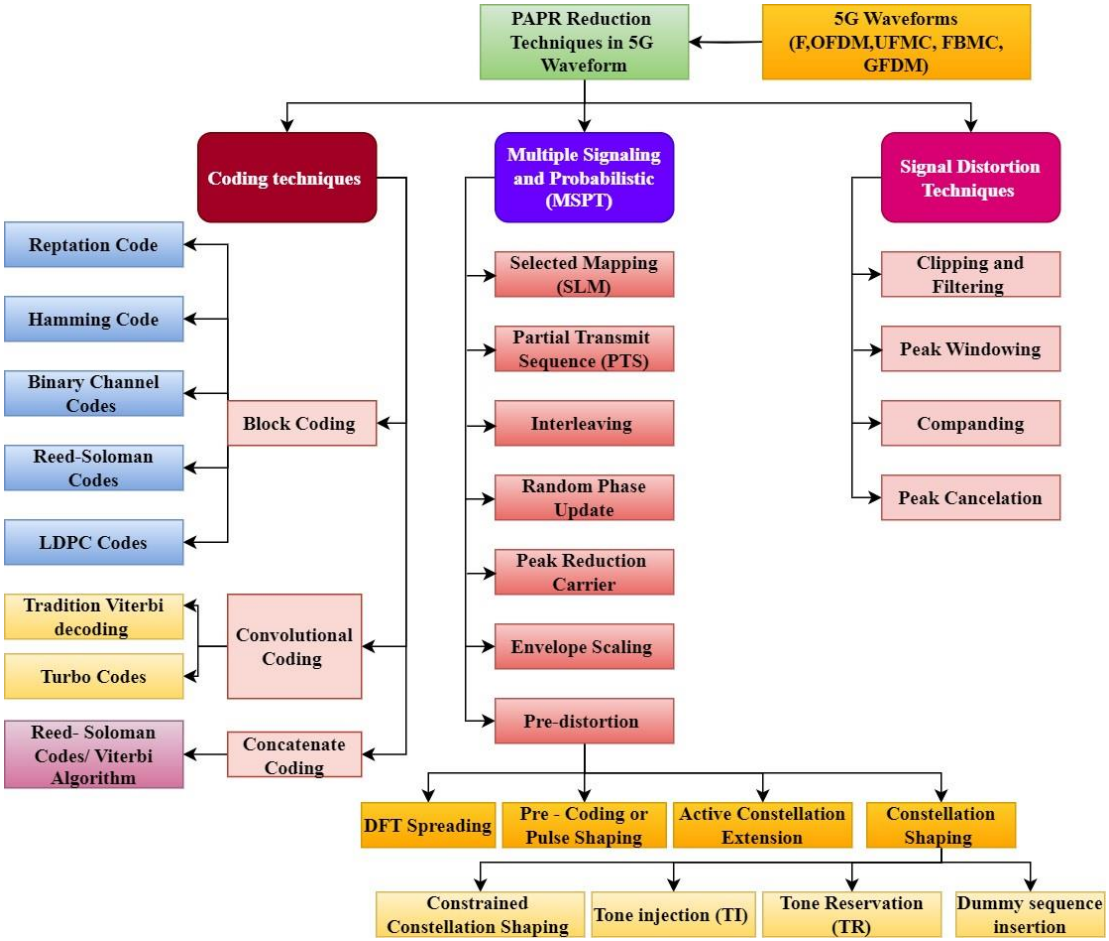

Figure 1. PAPR reduction techniques.

Since CP-OFDM signals likewise have prominent peaks, they are subject to the distortion technique known as companding [26]. M-law and A-law companding transforms are used to compress the OFDM signal and decrease PAPR while maintaining a manageable BER and minimal complexity [27, 28]. Probabilistic methods may also be used to alter the OFDM signal by adding or multiplying phase or optimization variables [29]. Selected Mapping (SLM) and SLM UFMC for the 5G waveform produce several OFDM symbols and then choose the one with the lowest PAPR[30]. Partial Transmit Sequences (PTS) are generated by slicing the OFDM symbol into independent subblocks [31, 32]. Moreover, combining them using weighted phase factors and finally selecting the phase factors such that the PAPR of the resulting signal is minimized. Any of these strategies may be coupled with others to form hybrid approaches that are tailored to the specifics of each system. Combining approaches like PTS with others like linear or non-linear companding [33] or SLM with PTS may minimize hardware and computational difficulties by lowering PAPR compared to using only one of these methods alone [34, 35].

One of the emerging waveform candidates for 5G networks is the UFMC system. High spectral efficiency is anticipated from UFMC because of its low latency, resistance to frequency offset, and suppression of radiation [36]. As was previously indicated, the UFMC system's multicarrier transmission technology benefits come at the expense of high PAPR [37, 38]. Therefore, in this research, it is suggested to combine the UFMC signals with a hybrid SLM-Mu Low companding. As a result, the hybrid SLM-Mu-low companding method's mathematical model is provided with an analysis of its PAPR, BER, and computing complexity. The performance of the approach in terms of the nonlinearity of the high-power amplifier is estimated using the Cubic Metric (CM) [39]. To determine how the power amplifier affects the signal, the CM is utilized in [40]. In conclusion, decreasing the number of candidates will decrease the reserved bits as side information and reduces the computational complexity at

the same time. Hence, it is worth controlling the number of candidates to get perfect results. Thus, there is a trade-off between the reduction performance and the computational complexity. Table I summarizes the previous related studies in the frequency domain, time domain, and the limitation of the applicable techniques.

TABLE I: SUMMARY OF THE IMPORTANT PREVIOUS WORKS

Author	Problem	Waveform	Method in Frequency domain	Method in Time domain	Method in hybrid domain	Limitations
(Sameh *et al.*)[41]	PAPR	UFMC	SLM			It produces a very high computational complexity and does not using cubic matric as evaluate
(Pooja *et al.*) [42]	PAPR	UFMC	SLM	Clipping, companding and (clipping &filtering)		It does not use cubic matric as evaluate and the PRV
(Rani *et al.*) [43]	PAPR	UFMC	SLM	clipping	SC-UFMC	It produces a very high computational complexity and does not using cubic matric as evaluate
(Deepa *et al.*) [44]	PAPR	OFDM	SLM			It does not use cubic matric as evaluate and the PRV and high complexity as well aa using IFFT adding to the system
(Pushkarev *et al.*) [45]	PAPR	OFDM	SLM	PTS	SLM-PTS	It produces a very high computational complexity and side information bits
(Satyavathi *et al.*) [46]	PAPR	OFDM	SLM	PTS	Applying (IDHT) on the hybrid algorithm (SLM-PTS)	It produces a very high computational complexity and side information bits
(Singh *et al.*) [47]	PAPR	OFDM	SLM	PTS	SLM-PTS	It produces a high computational complexity and side information bits
(Wang *et al.*) [48]	PAPR	OFDM	SLM	PTS	SLM-PTS	It produces a high computational complexity and side information bits
(Tiwari *et al.*) [49]	PAPR	OFDM	SLM	PTS	SLM-PTS	Its PAPR performance is lower than that of PR-PTS and does not using cubic matric as evaluate

TABLE II. LIST OF ACRONYMS

Adjacent channel leakage ratio	ACLR
Bit Error Rate	BER
Complementary Cumulative Distributive Function	CCDF
Cubic Metric	CM
Cyclic prefix-orthogonal frequency division multiplexing	CP-OFDM
Filter Bank Multicarrier	FBMC
Frequency division multiplexing	FDM
Filtered Orthogonal Frequency Division Multiplexing	F-OFDM
High-Power Amplifier	HPA
Inverse Discrete Fourie Transform	IDFT
Long-Term Evolution	LTE
Orthogonal frequency division multiplexing	OFDM
Peak-to-Average Power Ratio	PAPR
Physical Resource Block	PRB
Partial Transmit Sequences	PTS
Raw Cubic Metric	RCM
Selected Mapping	SLM
Quality of Service	QoS
Universal Filtered Multicarrier	UFMC
Wide-Code Division Multiple Access	W-CDMA

Finally, Table II presents the list of acronyms. This article is structured as follows. In Section II, the details of the resources and procedures are presented. In Section III, the mathematical models of the suggested procedure SLM-UFMC are laid out. Section IV presents the findings and discussion. Section V presents the study's findings and suggestions for further investigation.

II. Substances and Techniques

A. Conditions for the Experimental Model

The simulation's experimental experiments hope to boost 5G performance by reducing PAPR. It is recommended to use the Hybrid Method SLM-Mu low UFMC to identify the optimal wave with the minimum PAPR and CM. After that, the Hybrid Method SLM-Mu low UFMC is compared to the results of a simulation program testing three different waveforms. In Fig. 2, the primary procedures for implementing the simulation of the Hybrid Method SLM-Mu low UFMC and the other waveforms are shown. The core of the simulation model is made up of five distinct parts.

To begin, simulation environments are built using the Parameter sitting for the simulation. The core features of 5G, such as data rate, packet size, and the number of devices, are all included in this module. In the second place, the 5G waveform (UFMC, CP-OFDM), and then the implementation of the Hybrid Method SLM-Mu low UFMC model and the already existing UFMC and Hybrid Method SLM-Mu low-CP-OFDM models. Multiple solution-tracking windows have been included with this component [50].

To evaluate the performance of the proposed model in comparison with the tested waveforms, testing scenarios with varying states are generated using a range of QAM counts (e.g., 4, 8, 16, 64, 256). In each iteration of a given waveform, the situations are varied slightly. In the Evaluation metric section, the Hybrid Method SLM-Mu-UFMC, Mu-low UFMC, Mu-low CP-OFDM, Hybrid Method SLM-Mu-CP-OFDM, and traditional UFMC and CP-OFDM are compared using the performance metrics of CCDF and BER. Finally, windows-based graphs of the findings and visualizations are shown.

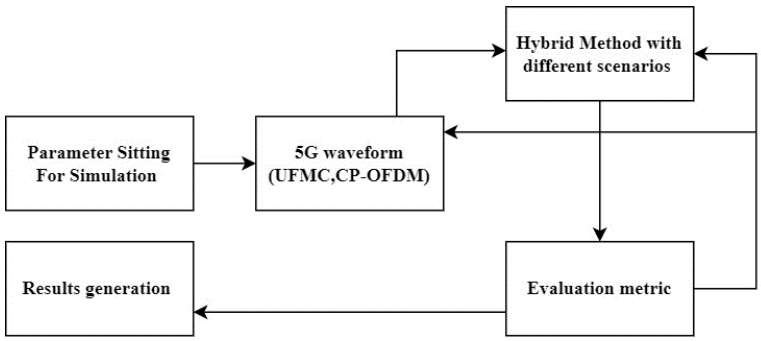

Figure 2. Simulation design-Please provide higher resolution figures

B. The Criteria for Assessment

The PAPR of a Complementary Cumulative Distributive Function (CCDF) is the likelihood that the CCDF has a positive expected value [51].

$$PAPR = 10\log_{10}\left[\frac{\max|x(k)|^2}{E[|x(k)|^2]}\right] \quad (1)$$

where $E[|x(k)|^2]$ is the mathematical operation that, when applied to the signal $x(k)$, yields its mean strength. High peaks delivered into the high-power amplifier (HPA) will cause it to enter its saturation area, leading to system damage. This means that the peaks can't be too steep. New evidence suggests that the PAPR measure cannot reliably forecast HPA power de-rating; as a result, the 3GPP has moved to a new metric, the cubic metric (CM) [52].

$$CM = \frac{20\log_{10}\{rms[x^3_{norm}(k)]\} - 20\log_{10}\{rms[x^3_{ref}(k)]\}}{K}\ dB \quad (2)$$

The RCM of a Wide-Code Division Multiple Access (W-CDMA) speech signals is represented by the expression where $20\log_{10}\{rms[x^3_{norm}(k)]\}$ is the raw cubic metric (RCM) of the signal $x(k)$ and $20\log_{10}\{rms[x^3_{ref}(k)]\}$ is a constant reference. It was determined that the reference signal was 1.25 dB [53]. The numerator represents a wide variety of signals suggested for LTE applications, while the denominator is the empirical slope factor, which is found experimentally to be 1.56. Additionally, $rms(x)$ may be determined by

$$rms(x) = \sqrt{\frac{\mathbf{x}^{\wedge}\mathbf{x}}{N}} \quad (3)$$

and

$$x_{norm}(k) = \frac{|x(k)|}{rms(x(k))} \quad (4)$$

In Eqs. (1-4), x represents the signal in its vector form. In other words, power de-rating describes how HPA power reduction impacts system performance. Adjacent channel leakage ratio (ACLR) is the ratio of the mean power allocated to a given channel to the mean power assigned to an adjacent channel [54]. This ratio is caused by the nonlinearity of the HPA. It has been determined that an ACLR of 30dB is necessary for effective functioning in

LTE systems [55]. The HPA operation is worth introducing to provide context for the preceding topic.

$$v_o(t) = G_1 v_i(t) + G_3 v_i^3(t) \quad (5)$$

where G1 and G2 represent the linear and cubic gain, respectively, of the power amplifier's intended layout. A power amplifier's power de-rating is the amount of power cutback needed to fulfill the transmitting system's ACLR criteria. Thus, the nonlinearity source in the power amplifier, the primary cause for the ACLR, is revealed by the second term in the final equation. Assuming the final expression's input to the HPA contains two adjacent frequencies:

$$x_{1,2}(k) = A_1 e^{j\theta_1} + A_2 e^{j\theta_2} \quad (6)$$

where $\theta_1 = 2\pi k \frac{a}{N}$ and $\theta_2 = 2\pi k \frac{b}{N}$ are the two sets of matching constellations point data, a and b are two nearby frequency indices. Finally, the formula for the two neighboring frequencies is

$$\begin{aligned} x_{1,2}(k) = G_1\left[A_1 e^{j\theta_1} + A_2 e^{j\theta_2}\right] \\ + G_3\left[A_1 e^{j\theta_1} \right. \\ \left. + A_2 e^{j\theta_2}\right]^3 \end{aligned} \quad (7)$$

Then adding a cube to the word leads to:

$$\begin{aligned} x_{1,2}(k) = G_1\left[A_1 e^{j\theta_1} + A_2 e^{j\theta_2}\right] \\ + G_3\left[A_1^3 e^{j3\theta_1}\right. \\ + A_2^3 e^{j3\theta_2} \\ + 3A_1^2 A_2 e^{j(2\theta_1+\theta_2)} \\ \left. + 3A_1 A_2^2 e^{j(\theta_1+2\theta_2)}\right] \end{aligned} \quad (8)$$

The linear basic signal frequencies are denoted by the first phrase, while the nonlinear frequencies are denoted by the second. Therefore, in the final expression, the words $3A_1^2 A_2 e^{j(2\theta_1+\theta_2)} + 3A_1 A_2^2 e^{j(\theta_1+2\theta_2)}$, which do not take into account any other terms that could have an influence, are the major impetus to ACLR [56]. This intermodulation occurs because of the $2\theta_1 + \theta_2$ and $\theta_1 + 2\theta_2$ frequencies generated by the cubic terms. In a nutshell:

$$\begin{aligned} & x(k) \\ & = G_1 \sum_{n=0}^{N-1} X_n e^{j2\pi k\frac{n}{N}} \\ & + G_3 \sum_{n=0}^{N-1} \left(X_n^3 e^{j2\pi k\frac{3n}{N}} + X_{n+1}^3 e^{j2\pi k\frac{3n+3}{N}}\right) \\ & + 3G_3 \sum_{n=0}^{N-1} \sum_{c=1}^{N-n-1} \left(X_n^2 X_{n+c} e^{j2\pi k\frac{n-c}{N}}\right. \\ & \left. + X_n X_{n+c}^2 e^{j2\pi k\frac{n+2c}{N}}\right) \end{aligned} \quad (9)$$

Using Eqs. (8-9), we find that the third intermodulation component is the true origin of ACLR. As a result, the cubic metric will provide more precise results for calculating the power back-off of power amplifiers than the PAPR measure would.

The BER is the ratio of the number of errors (N_{Er}) to the total number of bits transported (N_{bits}) throughout the period under study ($BER = N_{Er}/N_{bits}$). It is often represented as a percentage but has no standard unit of measurement [57].

III. Calculations and Modelling

A. Modeling the UFMC System

Based on the original OFDM system, UFMC may be thought of as a more generalized OFDM. This OFDM scheme is under consideration:

$$x(k) = \frac{1}{\sqrt{N}} \sum_{n=0}^{N-1} X(n) e^{j2\pi\frac{nk}{N}} \quad (10)$$

The final formula contains the OFDM signal, denoted by x, as an IDFT of dimension N, with k denoting the time domain and n the frequency domain. Quadrature multi-level amplitude modulation, often known as so-called M-QAM mapping, generates a random value for X. Mathematically, CP-OFDM without the cyclic prefix may be produced by applying a filter to the whole band; take into account the matrix format of Eq. (10):

$$\mathrm{x} = \mathrm{W} \cdot \mathrm{X} \quad (11)$$

where W is a NN IDFT matrix and N is the total number of subcarriers. When filter Eq. (12) is put into action, the resulting CP-OFDM is:

$$\mathrm{x} = \mathrm{F} \cdot \mathrm{W} \cdot \mathrm{X} \quad (12)$$

where F is the Toeplitz matrix of the finite impulse response (FIR) filter that performs the convolution across the N-subcarrier band. The UFMC system may be accessed if the whole band is split into R sub-bands [57]:

$$\mathrm{x} = \sum_{r=1}^{R} \mathrm{F}_r \cdot \mathrm{W}_r \cdot \mathrm{X}_r \quad (13)$$

where the M-QAM symbol entries of Xr are first transformed into the time domain following the column of the IDFT matrix Wr that corresponds to the requested frequency subband r, the UFMC system shown in Fig. 2 is defined by the final statement. The finalized mapping strategy is then presented and incorporated into the UFMC platform. However, the filter length is very important for the system's architecture. For example, the system simplifies to FBMC if the filter length P1 and X includes a single M-QAM symbol. Doing the filtering procedure in blocks eliminates the drawbacks of FBMC and allows for greater leeway in terms of system design and performance. In LTE parlance, a block-wise allocation is made using a physical resource block (PRB).

B. Strategies for Lowering PAPR

1) The SLM system based on the UFMC architecture

One effective frequency-domain method for lowering PAPR in OFDM systems is the SLM procedure. The basic idea is to generate B duplicates of the M-QAM modulating data vector, blend them elementwise with phase rotational vectors to get B applicants, perform an IDFT on each applicant, and then choose the one with the lowest PAPR (as computed after the IDFT block). B phase rotation vectors must be orthogonal to each other, and the phase rotation vectors are selected such that element-wise multiplications of any two elements of the vector do not exhibit a periodic pattern [58]. That is, after including the phase rotation vector, X_r in Eq. (14) looks like this:

$$\mathrm{X}_r^b = \mathrm{p}^b \times \mathrm{X}_r \tag{14}$$

where

$$\mathrm{X}_r^b = \begin{bmatrix} X_{r,0}^b \\ X_{r,1}^b \\ \vdots \\ X_{r,N-1}^b \end{bmatrix}, \quad \mathrm{p}^b = \begin{bmatrix} p_0^b & 0 & \cdots & 0 \\ 0 & p_1^b & \cdots & 0 \\ \vdots & \vdots & \ddots & 0 \\ 0 & 0 & \cdots & p_{N-1}^b \end{bmatrix}, \mathrm{X}_r = \begin{bmatrix} X_{r,0} \\ X_{r,1} \\ \vdots \\ X_{r,N-1} \end{bmatrix} \tag{15}$$

Additionally, b represents the p index of the stage rotational vector. Then, we can write down the UFMC-based SLM as,

$$\mathrm{x}^b = \sum_{r=1}^{R} \mathrm{F}_r \cdot \mathrm{W}_r \cdot [\mathrm{p}^b \times \mathrm{X}_r] \tag{16}$$

or

$$\mathrm{x}^b = \sum_{r=1}^{R} \mathrm{F}_r \cdot \mathrm{W}_r \cdot \mathrm{X}_r^b \tag{17}$$

To rephrase, because UFMC-based SLM is currently producing B applicants, the one with the lowest PAPR will be chosen for further transmission. Statistical difficulty in the situation shown in (17) above may be estimated as a regular CP-OFDM case [59]. For example, the CP-OFDM shares the same amount of complex multiplication and addition operations as the UFMC. This means that the total number of complex multiplications is:

$$\mu = \frac{N}{2}\log_2(N) \tag{18}$$

While we may express the total number of complicated additions as[59]:

$$\alpha = N\log_2(N) \tag{19}$$

To rephrase, the SLM scheme, which represents the PAPR/CM reduction strategy, will lead to an increase in the total amount of complicated operations for multiplication proportional to B, the number of applicants:

$$\mu_{SLM} = B\frac{N}{2}\log_2(N) \tag{20}$$

To get the entire amount of SLM candidates, we use the following equation:

$$\alpha_{SLM} = BN\log_2(N) \tag{21}$$

The SLM approach, in contrast, is a stochastic method; as a result, the BER will be unaffected; the more serious computing difficulty is a price worth paying for the very intriguing results. However, for the data to be retrieved, SLM must provide additional details to the receiver. There are just a few pieces of supplementary data, and they may be deduced as follows:

$$\delta = \log_2(B) \tag{22}$$

In other words, reducing the number of applicants simultaneously decreases computing complexity by reducing the number of bits reserved as side information. Therefore, limiting the pool of potential applicants might provide better outcomes. As a result, there is a trade-off between reduction efficiency and computational burden.

2) System for compiling logarithmic laws using Data from the UFMC

a) law commanding

A linear portion of the compressor characteristic is used for low-level inputs, while a logarithmic portion is used for high-level inputs in this compacting technique. Characteristics of the A-law compressor for a range of A values. At the value A=1, the quantization is uniform, and the characteristic is linear (no compression). The beginning of an A-law is midrise. Therefore, it must have a value other than zero [60]. "A" has a useful value of 87.6 in everyday situations. PCM telephone systems use the A-law coding scheme [61]. The characteristic's linear portion corresponds to low-level inputs, while the logarithmic portion applies to high-level inputs. The primary drawback of OFDM and UFMC may be mitigated with this method.

$$\mathrm{y(x)} = \begin{cases} \mathrm{y}_{max}\dfrac{\frac{A|\mathrm{x}|}{\mathrm{xm2x}}}{(1+\mathrm{A})}\,\mathrm{sgn}\,(\mathrm{x}) & 0 < \dfrac{|\mathrm{x}|}{\mathrm{x}_{max}} \le \dfrac{1}{\mathrm{A}} \\ \mathrm{y}_{max}\dfrac{[1+\log_e[\frac{A|\mathrm{x}|}{\mathrm{xm2x}}]]}{(1+\log_e \mathrm{A})}\,\mathrm{sgn}\,(\mathrm{x}) & \dfrac{1}{\mathrm{A}} < \dfrac{|\mathrm{x}|}{\mathrm{x}_{max}} \le 1 \end{cases} \tag{23}$$

where

- X = Signal input.
- Y = Final result or output signal.
- Input sign (X) may be positive (+) or negative (-) values.
- This is the absolute value of X, written as |X|.

- (Consultative Committee for International Telephony and Telegraphy) CCITT defines A as = 87.6.

b) μ-law aggregation method

The compression feature in -law expanding is non-uniform; it has a linear portion for low-level inputs and an exponential portion for high-level inputs. The features of the -law compressor are shown for a range of values in Figs. 5-15. The compressed level increases as it increases. Linearity (no reduction) in the characteristic is seen at =0, which is consistent with a uniform quantization. The root of -law is mid-tread. Consequently, its value is zero. "Has a practical value of 255[62].

Using the -Law encoding features, we may characterize the signal as:

$$y(x) = V\frac{\log(1+\mu\frac{|x|}{V})}{\log(1+\mu)}\operatorname{sgn}(x) \quad (24)$$

where V represents the maximum amplitude of the signal and x represents its instantaneous amplitude. Simply said, decompression is Eq. (24), backward. While the resolution of big signals is reduced, the resolution of tiny signals is improved by compression. Since peaks occur less often, the impact of the quantization noise due to the loss in resolution of the peaks is quite minimal. The compression mechanism presented here works by boosting weaker signals while leaving stronger peaks alone [63].

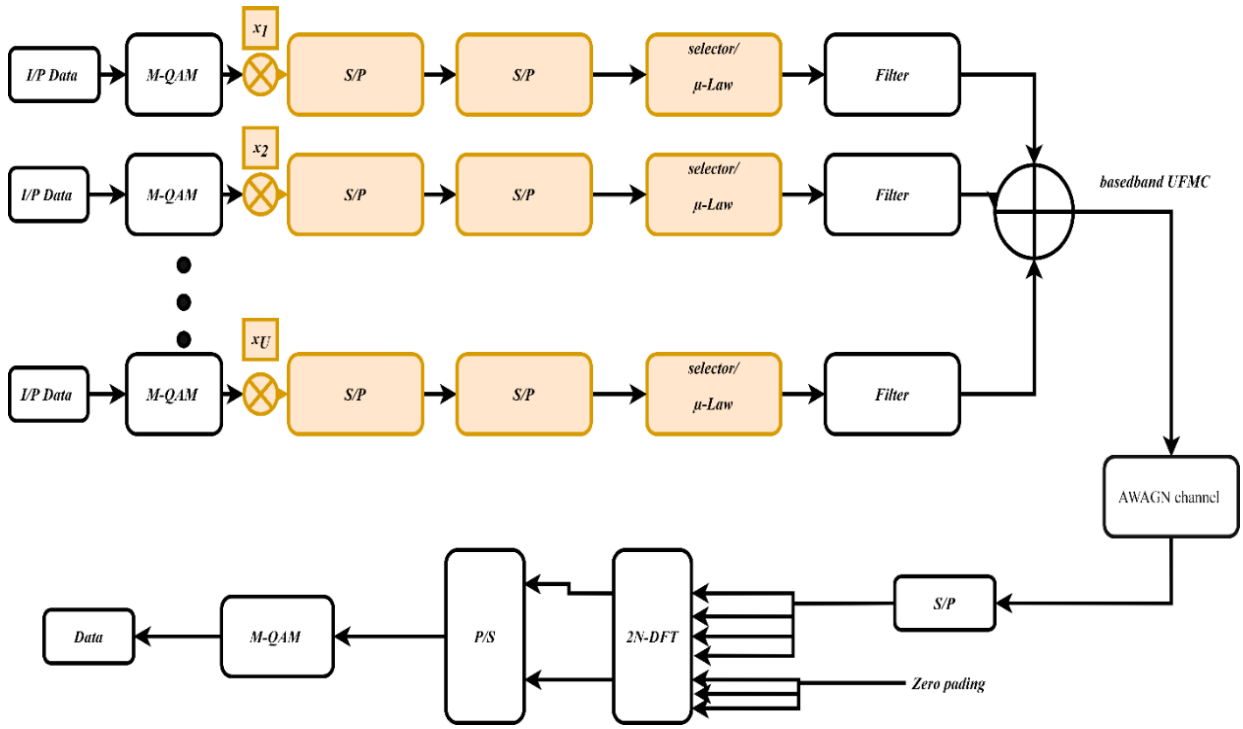

Figure 3. The proposed Universal Filtered Multicarrier (UFMC) baseband transceiver.

Fig. 3 depicts the suggested approach, which is a combination of SLM and companding methods. QAM (41.664256) keying technique is employed in this proposed approach to map the algorithm for the high data rate signal stream. The phase factors (4, 6, 8) are multiplied by the mapped signal at each subblock. Separate subblock signals are transformed into a single time-domain subblock UFMC signal. The -Law companding method is used to compress the subblock-UFMC signal. Finally, the best PAPR is chosen. Due to the lack of signal distortion introduced by the SLM mapping method, BER performance is not affected. But the complexity of the communication infrastructure is expected to grow. The companding method improves PAPR performance with little added complexity by amplifying the weak signal while dampening the strong one. The computational difficulty of μ-Law compression is said to vary with the encoding μ order.

$$\mu_{companding} = \frac{N}{2}\log_2(N) \quad (25)$$

$$\alpha_{companding} = N\log_2(N) \quad (26)$$

$$\mu_{low\ complexity} = \log_2(\mu) \quad (27)$$

IV. Results and Discussion

In this paper, four different scenarios are presented, each of which is carried out in the order M of the constellation. Table I provides a quick overview of the simulation settings utilized in what follows. According to Table I, there are 20 PRBs, and each PRB has 14 subcarriers, with QPSK, 16 QAM, 64 QAM, and 256 QAM being used to modulate each subcarrier. This results in 2, 4, 6, and 8 binary bits being sent in each of the four cases. These settings are chosen in compliance with LTE specifications. In addition, there are 4, 6, and 8-PRVs in each possible outcome. To further lessen processing and

complexity, the value of the -law companding is set to 6. The results of the simulation using 4-PRV and QPSK mapping are shown in Fig. 4a-b. These values correspond to the first-line entries in Table III.

The first case in Table III has a PRV of 4 and a modulation order of QPSK/4QAM. Fig. 4a shows that using the companding technique, the CCDF/CM is

reduced from 7.375dB to 3.5dB using traditional UFMC and to 6.5dB and 3.375dB using CP-OFDM. The μ-law is 6 orders. Surprisingly, frequency-time-domain CCDF/CM reduction method, as shown in Fig. 4a, SLM-companding was found the conventional UFMC and CP-OFDM reduce the CCDF/CM from 7.375dB to 3.875dB and 6.5dB and 3.625dB, respectively. According to the BER result, as shown in Fig. 4b, the BER for the UFMC and CP-OFDM is increased when using the companding method. On the other hand, the BER for UFMC and CP-OFDM is decreased when using the SLM- companding technique due to the SLM being a distortion-less technique. Whereas the complexity of the system is increased due to the side information.

TABLE III. SIMULATION PARAMETERS FOR SLM-M-LAW-CP-ORTHOGONAL FREQUENCY DIVISION MULTIPLEXING (OFDM), SLM-M-LAW-UFMC, AND CONVENTIONAL CP-OFDM AS WELL AS UFMC

N Size of IFFT	*No. of Subcarriers*	*No. of PRB*	*No. of PRV*	*-μ-law*	*M Constellation Order*
512	14	20	4, 6, and 8	6	4
512	14	20	4, 6, and 8	6	16
512	14	20	4, 6, and 8	6	64
512	14	20	4, 6, and 8	6	256

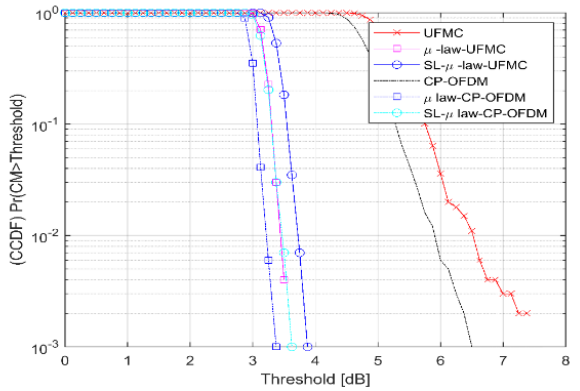

A. CCDF/CM

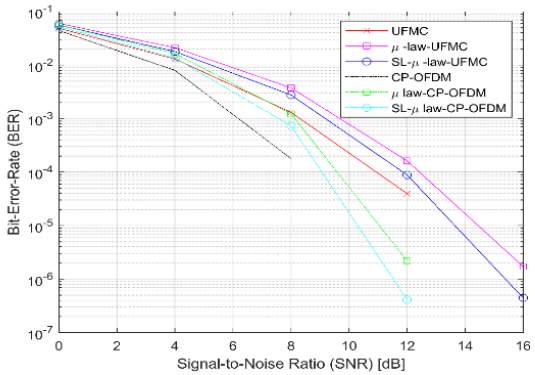

B. BER

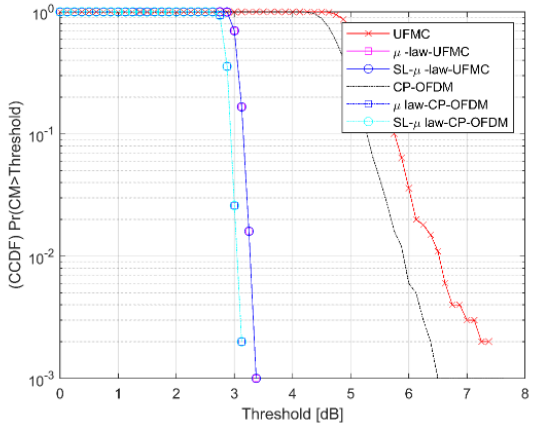

A. CCDF/CM

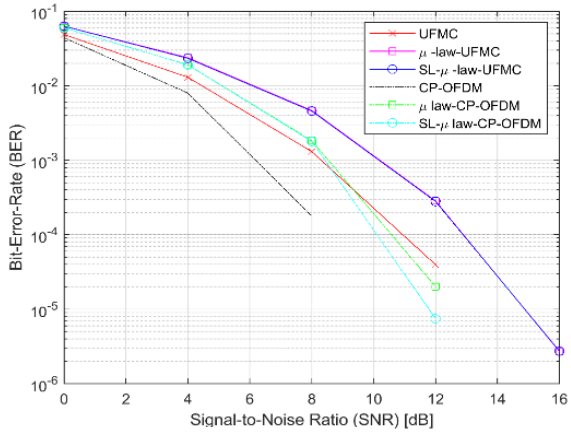

B. BER

Figure 5. The 4-QAM, 6-μ-law, and 6-PRV results of scenario 1

Six PRV were used in a setting where four PRV were used for QPSK/4QAM. Fig. 5a shows that the CCDFCM for CP-OFDM is 6.5dB, whereas that of standard UFMC is 7.375 dB. The CCDF\CM for UFMC and CP-OFDM with the SLM-companding technique is reduced to 3.375 dB and 3.125dB, with a reduction of 4dB and 3.375dB, respectively. At the same time, the performance for the companding does not change due to no change for the parameter related to the companding method.

For more accuracy in the result for the system, the BER performance is the same performance for μ-law-UFMC and SLM-μ-law UFMC as well as CCDF\CM performance. Mean that it could make the tard-off between the CCDF\CM performance, BER performance, and the complexity of the system.

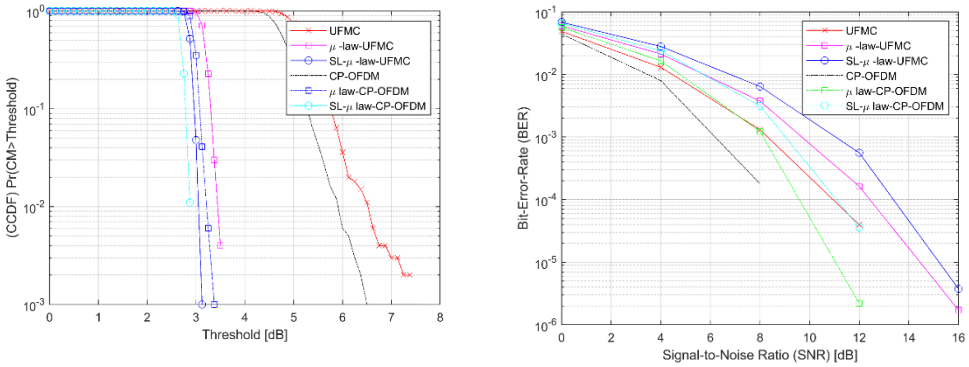

A. CCDF/CM **B. BER**

Figure 6. The 4-QAM, 6-μ-law, and 8-PRV results of scenario 1.

In the last case in the first scenario, the PRV order increased to 8. In Fig. 6a, the CCDF/CM for SLM-companding UFMC and CP-OFDM is reduced from 6.125dB to 3.125dB and 5.875dB to 2.875dB, respectively. According to Fig. 6b, the BER SLM-companding UFMC and CP-OFDM had better performance when increasing the SNR. In conclusion, Table II together mentions the three cases for the first scenario results with those obtained. To be fair, the best optimization, according to Table IV, when using the QPSK /4QAM,6PRV, and 6 order μ-law companding.in addition, low complexity and suitable BER compare with other cases.

TABLE IV. COMPILING UFMC AND CP-OFDM, SLM — LAW UFMC AND CP-OFDM, AND CONVENTIONAL UFMC AND CP-OFDM SIMULATION RESULTS FOR THE FIRST SCENARIO (QPSK/4-QAM)

Waveform	No. of PRV	CCDF/CM Before Reduction in dB	CCDF/CM μ-law After Reduction in dB	CCDF/CM SL- μ-law After Reduction in dB	CCDF/CM μ-law Reduction in dB	CCDF/CM SL- μ-law Reduction in dB
CP-OFDM	4	6.5	3.375	3.625	3.125	2.875
UFMC	4	7.375	3.5	3.875	3.875	3.5
CP-OFDM	6	6.5	3.125	3.125	3.375	3.375
UFMC	6	7.375	3.375	3.375	4	4
CP-OFDM	8	5.875	3.25	2.875	2.625	3
UFMC	8	6.125	3.5	3.125	2.625	3

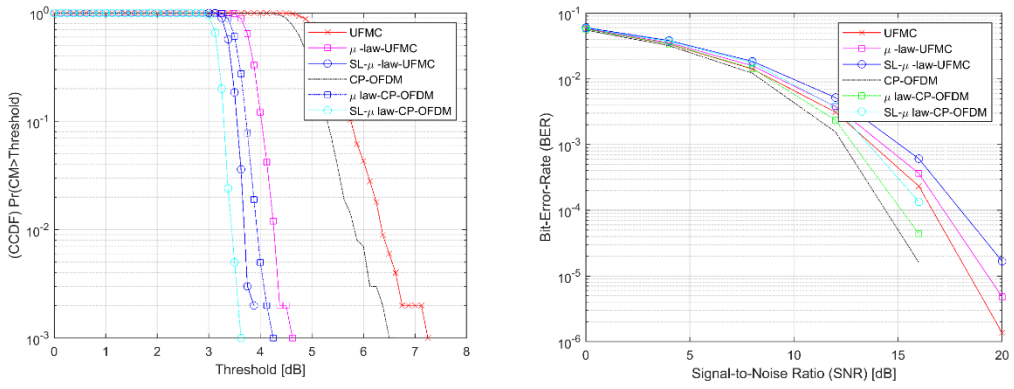

A. CCDF/CM **B. BER**

Figure 7. The 16-QAM, 6-μ-law, and 4-PRV results of scenario 2 .

The increased modulation order to 16QAM with four PRV was used in the second scenario in both 5G waveforms. Both performance reduction of SLM-companding UFMC and SLM-companding CP-OFDM were more efficient than the μ-law companding performance. The conventional UFMC and CP-OFDM reduce the CCDF/CM for SLM-companding shown in Fig. 7a from 7.25dB to 4.625dB and 6.5dB to 4.25dB, respectively. On the other hand, in Fig. 7a, the SLM-companding UFMC and CP-OFDM are reduced from 7.25dB to 3.9dB and 6.5dB to 3.625 dB. Generally, the performance of reduction for UFMC when increasing the order of modulation is more efficient than the CP-OFDM in both techniques. According to Fig. 7b, the BER performance, when increasing the SNR, the UFMC better CP-OFDM. In addition, the UFMC is more suitable for the short burst, which means that the User is near the Base station.

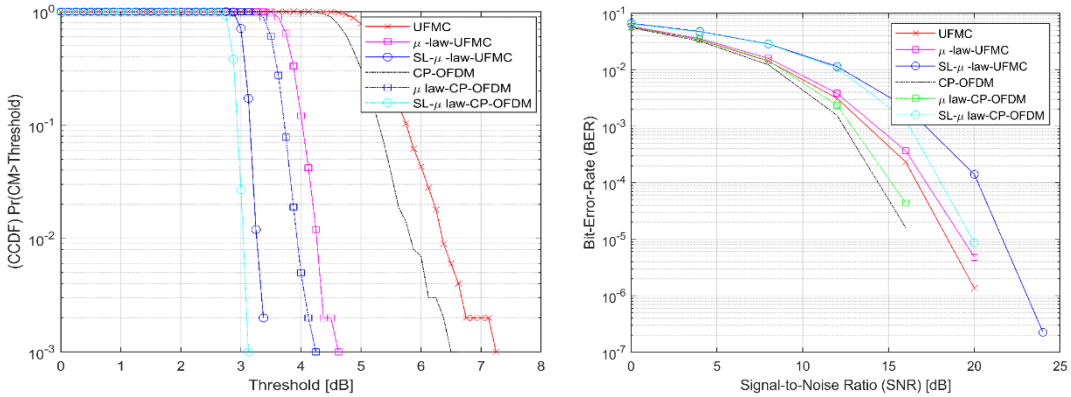

A. CCDF/CM **B. BER**

Figure 8. The 16-QAM, 6-μ-law, and 6-PRV results of scenario 2.

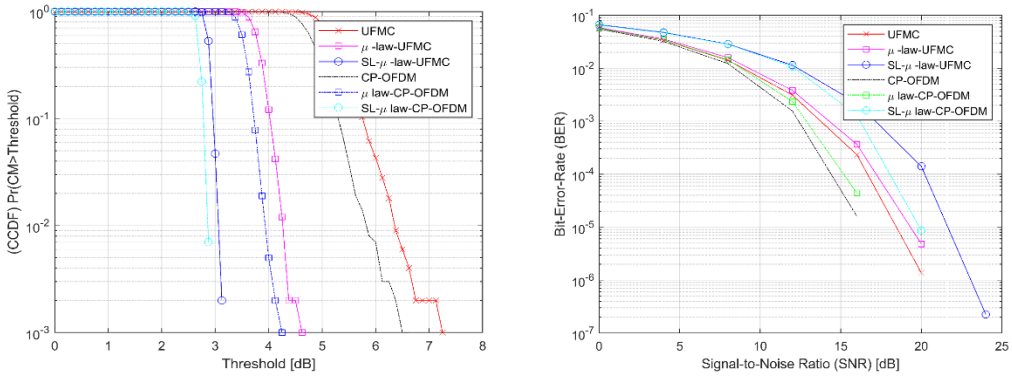

Figure 9. The 16-QAM, 6-μ-law, and 8-PRV results of scenario 2

A. CCDF/CM **B. BER**

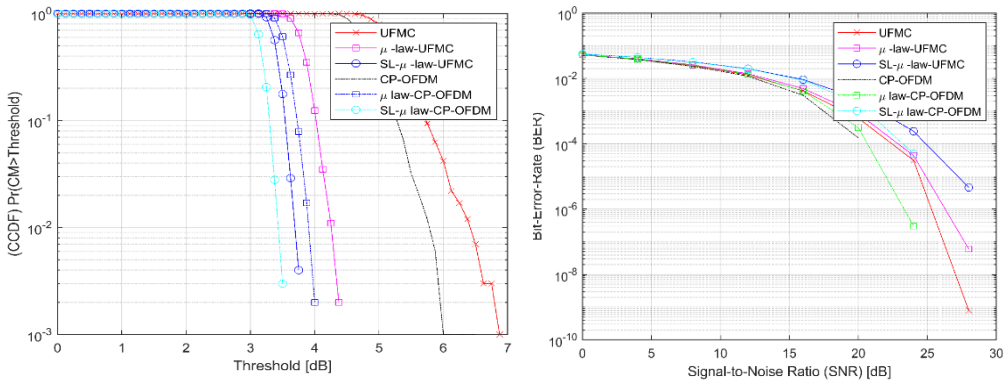

A. CCDF/CM **B. BER**

Figure 10. The 64-QAM, 6-μ-law, and 4-PRV results of scenario 3.

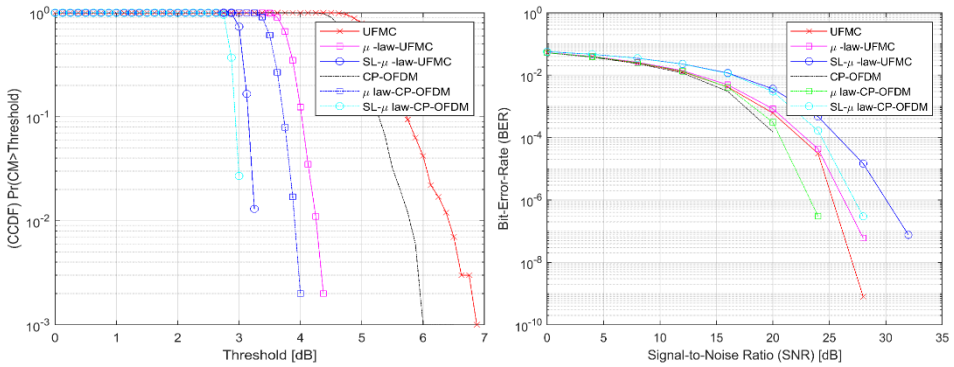

A. CCDF/CM **B. BER**

Figure 11. The 64-QAM, 6-μ-law, and 6-PRV results of scenario 3.

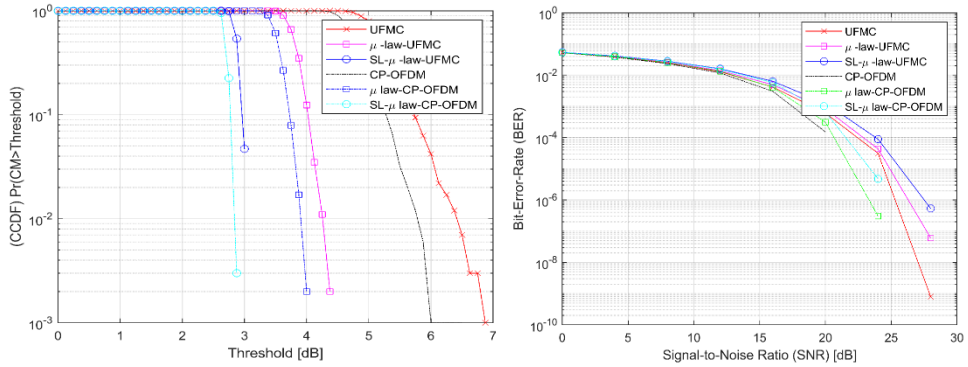

A. CCDF/CM **B. BER**

Figure 12. The 64-QAM, 6-μ-law, and 8-PRV results of scenario 3.

The simulation results for the last example in the second scenario are shown in Fig. 8a– Fig. 9a; this case uses 16-QAM with 6-8-PRV for the CCDF/CM. Fig. 8a shows a reduction in noise floor from 7.25 dB to 3.375 dB for CM SLM-companding UFMC and from 6.5 dB to 3 dB for CP-OFDM. Fig. 9a shows a reduction in noise from 7.25 dB to 3.375 dB and 6 dB to 2.875 dB when the PRV is raised. However, this does not affect the UFMC's performance. Increasing the PRV count eventually reduces CM but at the expense of added complexity. The results of the second set of situations are compiled in Table V. Compared to CP-OFDM, UFMC achieves superior performance reduction in both companding and SLM-companding.

TABLE V. SIMULATION RESULTS OF THE SECOND SCENARIO (16-QAM), COMPANDING UFMC AND CP-OFDM, SLM-M-LAW UFMC, AND CP-OFDM, AND CONVENTIONAL UFMC AND CP-OFDM

Waveform	No. of PRV	CCDF/CM Before Reduction in dB	CCDF/CM μ-law After Reduction in dB	CCDF/CM SL- μ-law After Reduction in dB	CCDF/CM μ-law Reduction in dB	CCDF/CM SL- μ-law Reduction in dB
CP-OFDM	4	6.5	4.25	3.625	2.25	2.875
UFMC	4	7.25	4.625	3.9	2.625	3.35
CP-OFDM	6	6.5	4.25	2.875	2.25	3.625
UFMC	6	7.25	4.625	3.375	2.625	3.875
CP-OFDM	8	6	4.25	2.875	1.75	3.125
UFMC	8	7.25	4.625	3.375	2.625	3.875

The third case provides a further improvement to the basebands-to-64-QAM mapping. In a broad sense, the importance of CM rose with the order of modulation. The achievement of the first case of this scenario is the 4-PRV which results in a CCDF/CM companding of UFMC and CP-OFDM as shown in Fig. 10a is 6.625dB to 4dB and 5.875dB to 6.625 to 4.375dB, respectively. On the other hand, the SLM-companding technique for UFMC and CP-OFDM reduces the CCDF/CM from 6.625dB to 4dB and 3dB to 6.625 to 3.5dB, respectively. Eventually, the SL- μ-law reduction is more efficient than the μ-law reduction with the UFMC waveform. According to Fig. 10b, the

worst performance of BER is the covenantal CP-OFDM, whereas the best BER performance is covenantal UFMC when increases the SNR. Fig. 11a and Fig. 12a show us clearly that when the modulation order is raised, so too must be the PRV. Fig. 11a demonstrates that the CM does not fare any better than the 4-PRV. Fig. 12a demonstrates how increasing the PRV results in a decrease in SLM-companding UFMC and CP-OFDM from 6.625dB to 3.75dB and from 5.875dB to 3.5dB, respectively.

Table VI. The SLM-companding technique for UFMC and CP-OFDM in all cases in this scenario has more reduction in the CM. Moreover, the SLM-companding technique for UFMC has a better reduction than the SLM-companding technique for CP-OFDM.

TABLE VI. SIMULATION RESULTS OF THE SECOND SCENARIO (16-QAM), COMPANDING UFMC AND CP-OFDM, SLM-M-LAW UFMC, AND CP-OFDM, AND CONVENTIONAL UFMC AND CP-OFDM

Waveform	No. of PRV	CCDF/CM Before Reduction in dB	CCDF/CM μ-law After Reduction in dB	CCDF/CM SL– μ– law After Reduction in dB	CCDF/CM μ-law Reduction in dB	CCDF/CM SL– μ – law Reduction in dB
CP–OFDM	4	5.875	4	3.5	1.875	2.375
UFMC	4	6.625	4.375	3.75	2.25	2.875
CP–OFDM	6	5.5	3.875	3	1.625	2.5
UFMC	6	6.125	4.125	3.25	2	2.875
CP–OFDM	8	5.375	3.75	2.75	1.625	2.625
UFMC	8	5.875	4.125	3	1.75	2.875

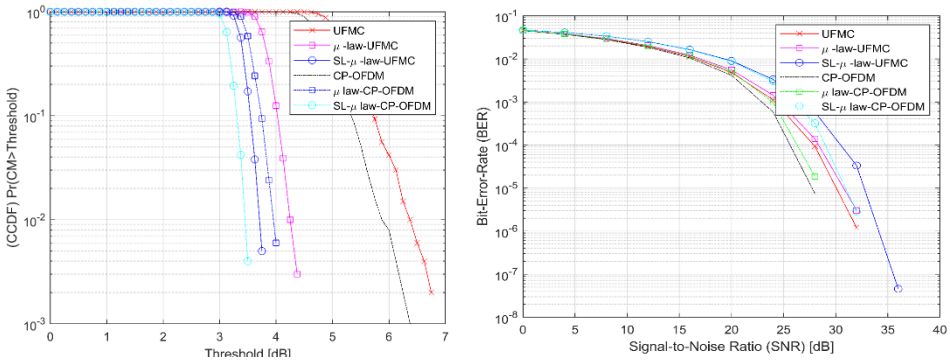

A. CCDF/CM **B. BER**

Figure 13. The 256-QAM, 6-μ-law, and 4-PRV results of scenario 4.

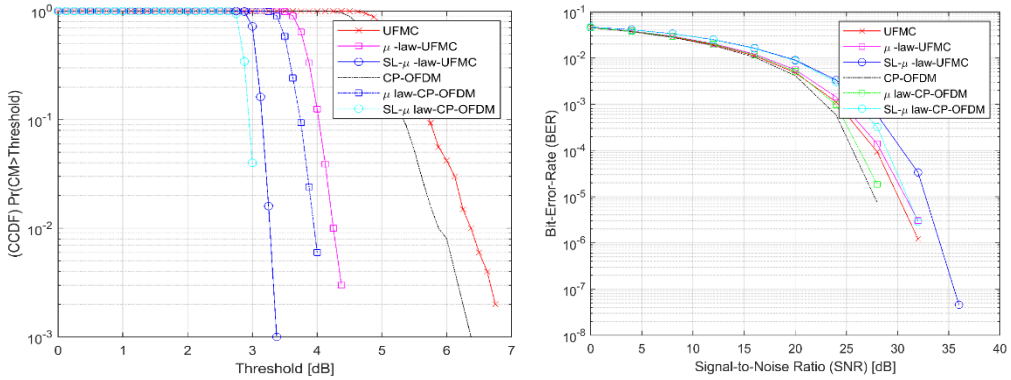

A. CCDF/CM **B. BER**

Figure 14. The 256-QAM, 6-μ-law and 6-PRV results of scenario 4.

In the third and final case, the 256-QAM modulation order increased, allowing for the use of 4, 6, and 8-PRV with a 6 μ-law companding order. Figs. 13–15a demonstrates that the UFMC may be lowered by 2.75dB, 2.75dB, and 3.375dB using the SLM-companding approach for 4-PRV, 6-PRV, and 8-PRV, respectively. However, as can be shown in Figs. 13–15, the UFMC is lowered by 2.25dB for 4-PRV, 1.875dB for 6-PRV, and 2.25dB for 8-PRV when compared to the -law case. Figs. 13–15a demonstrate that the CP-OFDM waveform is attenuated 2.75dB for 4-PRV, 2.375dB for 6-PRV, and 2.125dB for 8-PRV using SLM-companding method and μ-law companding. Table VII and VII when. displays the final scenario's outcomes.

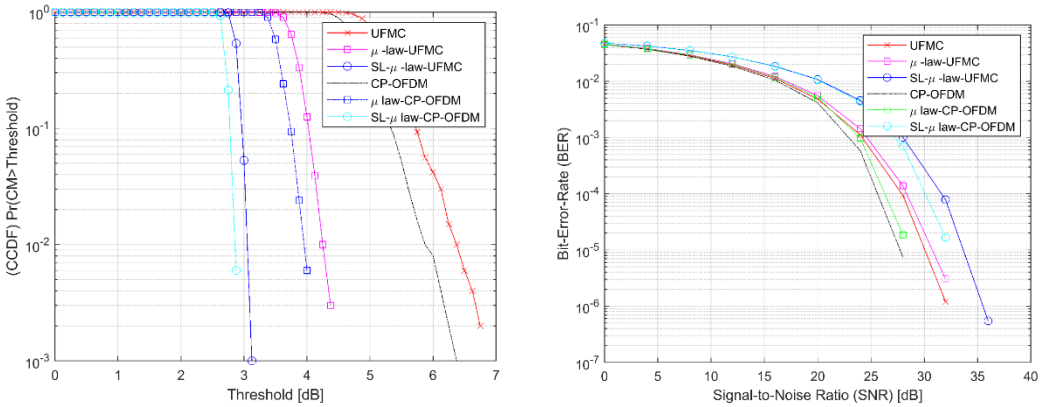

A. CCDF/CM **B. BER**

Figure 15. The 256-QAM, 6-μ-law, and 8-PRV results of scenario 4.

TABLE VII. SIMULATION RESULTS OF THE SECOND SCENARIO (16-QAM), COMPANDING UFMC AND CP-OFDM, SLM-M-LAW UFMC AND CP-OFDM, AND CONVENTIONAL UFMC AND CP-OFDM.

Waveform	No. of PRV	CCDF/CM Before Reduction in dB	CCDF/CM μ-law After Reduction in dB	CCDF/CM SL– μ– law After Reduction in dB	CCDF/CM μ– law Reduction in dB	CCDF/CM SL– μ– law Reduction in dB
CP–OFDM	4	6	4	3.5	2	2.5
UFMC	4	6.5	4.25	3.75	2.25	2.75
CP–OFDM	6	5.625	3.75	3.25	1.875	2.375
UFMC	6	6	4.125	3.25	1.875	2.75
CP–OFDM	8	6.125	4	2.87	2.125	3.255
UFMC	8	6.5	4.25	3.125	2.25	3.375

TABLE VIII. PERCENTAGE CM REDUCTION COMPARISONS OF THE UFMC AND CP-OFDM FOR ALL SCENARIOS

waveform	No. of PRV	CCDF/CM μ – law Reduction in % (QPSK/4QAM)	CCDF/CM SL– μ – law Reduction in % (QPSK/4QAM)	CCDF/CM μ – law Reduction in % (16-QAM)	CCDF/CM SL– μ– law Reduction in % (16-QAM)	CCDF/CM μ– law Reduction in % (64-QAM)	CCDF/CM SL– μ– law Reduction in % (64-QAM)	CCDF/CM μ – law Reduction in % (256 – QAM)	CCDF/CM SL– μ– law Reduction in % (256-QAM)
CP-OFDM	4	48%	44%	35%	44%	32%	40%	33%	42%
UFMC	4	53%	47%	36%	46%	34%	43%	35%	42%
CP-OFDM	6	52%	52%	35%	54%	30%	45%	33%	42%
UFMC	6	54%	54%	36%	53%	33%	47%	31%	46%
CP-OFDM	8	45%	51%	29%	52%	30%	49%	35%	53%
UFMC	8	43%	49%	36%	53%	30%	49%	35%	52%

However, the number of multiplies and sums required to minimize the CM values is proportional to the IFFT size and the number of candidates. However, there is a trade-off between the two factors. According to Table IX, the total number of multiplications performed in the situations ranged from 9219 for CP-OFDM or conventional UFMC to 18.435 for PRV SLM-companding -UFMC (using either 6 or 8 PRV SLMs). To get the total number of additions,

divide the sums given in Fig. 20-21. More candidates mean more supporting data, which adds to the burden. Where (22) specifies that the side information bits for a 4-PRV, 6-PRV, or 8-PRV are 2 and 3.

TABLE IX. PERCENTAGE CM REDUCTION COMPARISONS OF THE UFMC AND CP-OFDM FOR ALL SCENARIOS

N	B	δ	μ	μSLM companding	α SLM companding
512	4	2	6	9219	18435
512	6	3	6	13827	27651
512	8	3	6	18435	36867

Table X shows that in both the CP-OFDM and conventional UFMC cases, as well as the companding -UFMC and companding -CP-OFDM cases, the total number of multiplication operations was 2307. To get the total number of additions, divide the sums given in Eqs. (24-25) by 2. The overhead companding μ also rises when the low order grows in quantity. According to Eq. (27), the lowest order bit value for μ is 6.

TABLE X. CALCULATION OF THE COMPUTATIONAL COMPLEXITY OF THE COMPANDING UFMC

N	μ	μ companding	α companding
512	6	2307	4611

V. RECOMMENDATIONS FOR FUTURE WORK

It is highly recommended that more research be carried out in the following areas. The proposed methods are validated on the OFDM and F-OFDM systems. It is encouraged to apply the proposed methods to the other waveform design candidates, such as FBMC and UFMC. Further research is required to take into account the effect of the transmitter filter on the computational complexity, which should be studied in depth. The proposed methods have been applied to the F-OFDM system as a waveform candidate for the next generation to evaluate the PAPR reduction performance, so it is recommended to apply these methods to the FBMC and UFMC candidates to study the PAPR performance and the complexity level for these systems. The provided approaches and algorithms are used to apply the explicit side information to the UFMC and CP-OFDM systems. As a result, the information that the receiver uses to reconstruct the initial data comes from the side information. The ancillary information causes a reduction in the efficiency of the transmission. As a result, it is strongly suggested that new techniques be developed to transmit multicarrier signals without including side information. The recommended approaches for encoding the supplementary information bits into the transmitting signals need to be developed further by future researchers.

VI. CONCLUSION

The hybrid approach reduces hardware and computational demands by combining SLM with companding in the frequency and time domains. Previous research has recommended using the SLM technique to lower PAPR/CM in the UFMC waveform. The SLM adds computational complexity to find candidates for B due to the multiple signal representation. In addition, side details must be transmitted, which decreases the average rate of effective transmission of messages. It is also indicated that by decreasing PAPR, the hybrid technique improves HPA 's efficiency. This strategy is generalized to minimize PAPR by appending companding approaches such as μ-law. In this study, the μ-law companded CM of the μ-law technique is 3.375dB in low modulation order (4QAM). Besides, the value is 2.25 dB in high modulation order (256 QAM) is reduced without escalating hardware complexity. Using selected mapping has the benefit of reducing the PAPR / CM capabilities without compromising the BER performance of the system. Thus, the reduction benefit may be enhanced with the rise in the number of PRV, but at the cost of high computational complexity. The results of the tests show that the CCDF / CM may be reduced by 4 dB with the help of SLM companding in a 6-PRV scenario where the mapping order is 4-QAM. A CM loss of 3.875 dB is achieved using 16-QAM. In the end, 64-QAM achieves a CM reduction of 2.875 dB, whereas 256-QAM achieves a CM reduction of 3.375 dB. This study contributes by using the SLM-companding approach to lower the CM for the UFMC waveform at the expense of the BER. The approach has the drawback of not taking into account contextual details. Using a Dummy Sequence Insertion (DSI) to make use of ancillary data during a data transfer is something to think about for future development.

CONFLICT OF INTEREST

The authors declare no conflict of interest.

AUTHOR CONTRIBUTIONS

Farooq wrote the draft of the article. Lukman Audah supervised the research and revised the final draft. Sameer Alani and Ahmed Talaat reviewed the article. Mohammed Ahmed has updated and revised the language of the article. all authors had approved the final version.

FUNDING

The authors would like to extend their appreciation to the Faculty of Electrical and Electronic Engineering, University Tun Hussein Onn in Malaysia for supporting this research Acknowledgment.

REFERENCES

[1] M. Mounir, M. B. El-Mashade, S. Berra, G. S. Gaba, and M. Masud, "A novel hybrid precoding-companding technique for peak-to-average power ratio reduction in 5G and beyond," *Sensors*, vol. 21, no. 4, pp. 1–22, 2021.

[2] D. A. Aziz, R. Asgarnezhad, A. A. Saber, and S. Alani, "A developed IoT platform-based data repository for smart farming applications," *Journal of Communications*, pp. 187–197, 2023.

[3] S. Henry, A. Alsohaily, and E. S. Sousa, "5G is real: Evaluating the compliance of the 3GPP 5G new radio system with the ITU IMT-2020 requirements," *IEEE Access*, vol. 8, pp. 42828–42840, 2020.

[4] Q. V. Khanh, V. H. Nguyen, Q. N. Minh, A. Dang Van, N. Le Anh, and A. Chehri, "An efficient edge computing management mechanism for sustainable smart cities," *Sustainable Computing: Informatics and Systems*, vol. 38, p. 100867, Apr. 2023.

[5] Y. Ahn, W. Kim, and B. Shim, "Active user detection and channel estimation for massive machine-type communication: Deep learning approach," *IEEE Internet of Things Journal*, vol. 9, no. 14, pp. 11904–11917, 2022.

[6] L. Qiao, Y. Li, D. Chen, S. Serikawa, M. Guizani, and Z. Lv, "A survey on 5G/6G, AI, and robotics," *Computers and Electrical Engineering*, vol. 95, 2021.

[7] Y. I. Hammadi, R. K. Ahmed, O. A. Mahmood, and A. Muthanna, "New filtering method to reduce PAPR and OOBE of UFMC in 5G communication system," *Lecture Notes in Computer Science (including subseries Lecture Notes in Artificial Intelligence and Lecture Notes in Bioinformatics)*, pp. 3–16, 2022.

[8] F. S. Shawqi *et al.*, 'A new SLM-UFMC model for universal filtered multi-carrier to reduce cubic metric and peak to average power ratio in 5G technology," *Symmetry*, vol. 12, no. 6, 2020.

[9] E. Esenogho, K. Djouani, and A. M. Kurien, "Integrating artificial intelligence internet of things and 5G for next-generation smartgrid: A survey of trends challenges and prospect," *IEEE Access*, vol. 10, pp. 4794–4831, 2022.

[10] Q. V. Khanh, A. Chehri, N. M. Quy, N. D. Han, and N. T. Ban, "Innovative trends in the 6G Era: A comprehensive survey of architecture, applications, technologies, and challenges," *IEEE Access*, 2023.

[11] V. A. Dang, Q. Vu Khanh, V. H. Nguyen, T. Nguyen, and D. C. Nguyen, "Intelligent healthcare: Integration of emerging technologies and internet of things for humanity," *Sensors*, vol. 23, no. 9, 2023.

[12] M. Jaber, M. A. Imran, R. Tafazolli, and A. Tukmanov, "5G backhaul challenges and emerging research directions: A survey," *IEEE Access*, vol. 4, pp. 1743–1766, 2016.

[13] S. Sidiq, J. A. Sheikh, F. Mustafa, B. A. Malik, and I. B. Sofi, "A new genetic algorithm bio-inspired based impartial evaluation of UFMC and GFDM under diverse window constraints," *Arabian Journal for Science and Engineering*, vol. 47, no. 11, pp. 14173–14184, 2022.

[14] T. A. Abdulhussein, H. A. A. Falahi, D. A. Smait, S. Alani, S. N. Mahmood, and M. S. Mustafa, "Early coronavirus disease detection using internet of things smart system," *International Journal of Electrical and Computer Engineering (IJECE)*, vol. 13, no. 1, p. 1161, Feb. 2023.

[15] M. A. Saad *et al.*, "Total energy consumption analysis in wireless mobile ad hoc network with varying mobile nodes," *Indonesian Journal of Electrical Engineering and Computer Science*, vol. 20, no. 3, pp. 1397–1405, 2020.

[16] B. Hasan, S. Alani, and M. A. Saad, "Secured node detection technique based on artificial neural network for wireless sensor network," *International Journal of Electrical and Computer Engineering (IJECE)*, vol. 11, no. 1, p. 536, Feb. 2021.

[17] Y. A. Jawhar *et al.*, "A review of partial transmit sequence for papr reduction in the OFDM systems," *IEEE Access*, vol. 7, pp. 18021–18041, 2019.

[18] S. Alani, S. N. Mahmood, S. Z. Attaallah, H. S. Mhmood, Z. A. Khudhur, and A. A. Dhannoon, 'IoT based implemented comparison analysis of two well-known network platforms for smart home automation," *International Journal of Electrical and Computer Engineering (IJECE)*, vol. 11, no. 1, p. 442, Feb. 2021.

[19] H. Alkatrani *et al.*, 'Polygon number algorithm for peak-to-average ratio reduction of massive 5G systems using modified partial transmit sequence scheme," *Wireless Communications and Mobile Computing*, 2021.

[20] F. Sandoval, G. Poitau, and F. Gagnon, 'Hybrid peak-to-average power ratio reduction techniques: Review and performance comparison," *IEEE Access*, vol. 5, pp. 27145–27161, 2017.

[21] Y. L. Sit, B. Nuss, and T. Zwick, "On mutual interference cancellation in a MIMO OFDM multiuser radar-communication network," *IEEE Transactions on Vehicular Technology*, vol. 67, no. 4, pp. 3339–3348, 2018.

[22] S. Cha, M. Park, S. Lee, K. J. Bang, and D. Hong, "A new PAPR reduction technique for OFDM systems using advanced peak windowing method," *IEEE Transactions on Consumer Electronics*, vol. 54, no. 2, pp. 405–410, 2008.

[23] H. B. Jeon, J. S. No, and D. J. Shin, "A new PAPR reduction scheme using efficient peak cancellation for OFDM systems," *IEEE Transactions on Broadcasting*, vol. 58, no. 4, pp. 619–628, 2012.

[24] H. Bitra, P. Ponnusamy, S. Chintagunta, and S. Pragadeshwaran, "Nonlinear companding transforms for reducing the PAPR of OTFS signal," *Physical Communication*, vol. 53, 2022.

[25] T. Jiang and Y. Wu, "An overview: Peak-to-average power ratio reduction techniques for OFDM signals," *IEEE Transactions on Broadcasting*, vol. 54, no. 2, pp. 257–268, 2008.

[26] O. S. Al-Heety, Z. Zakaria, M. Ismail, M. M. Shakir, S. Alani, and H. Alsariera, 'A comprehensive survey: Benefits, services, recent works, challenges, security, and use cases for SDN-VANET," *IEEE Access*, vol. 8, pp. 91028–91047, 2020.

[27] O. R. Daoud, Q. J. Hamarsheh, and A. A. Damati, '5G wireless communications performance based on multiparallel processing algorithm for Papr reduction," in *Proc. 2022 19th IEEE International Multi-Conference on Systems, Signals and Devices, SSD 2022*, pp. 1329–1332, 2022.

[28] X. Huang, J. Lu, J. Zheng, K. B. Letaief, and J. Gu, "Companding transform for reduction in peak-to-average power ratio of OFDM signals," *IEEE Transactions on Wireless Communications*, vol. 3, no. 6, pp. 2030–2039, 2004.

[29] K. Mhatre and U. P. Khot, 'Efficient selective mapping papr reduction technique," *Procedia Computer Science*, vol. 45, pp. 620–627, 2015.

[30] H. Y. Liang, 'Selective mapping technique based on an adaptive phase-generation mechanism to reduce peak-to-average power ratio in orthogonal frequency division multiplexing systems," *IEEE Access*, vol. 7, pp. 96712–96718, 2019.

[31] N. Taşpinar, A. Kalinli, and M. Yildirim, 'Partial transmit sequences for papr reduction using parallel tabu search algorithm in OFDM systems," *IEEE Communications Letters*, vol. 15, no. 9, pp. 974–976, 2011.

[32] S. Thota, Y. Kamatham, and C. S. Paidimarry, "Analysis of hybrid papr reduction methods of OFDM Signal for HPA models in wireless communications," *IEEE Access*, vol. 8, pp. 22780–22791, 2020.

[33] S. R. Kondamuri and A. Sundru, 'Non linear companding transform to mitigate papr in DCT based SC-FDMA system," *Wireless Personal Communications*, vol. 112, no. 1, pp. 503–522, 2020.

[34] A. D. S. Jayalath and C. Tellambura, 'SLM and PTS peak-power reduction of OFDM signals without side information," *IEEE Transactions on Wireless Communications*, vol. 4, no. 5, pp. 2006–2013, 2005.

[35] S. A. Rashid, L. Audah, M. M. Hamdi, M. S. Abood, and S. Alani, 'Reliable and efficient data dissemination scheme in VANET: A review," *International Journal of Electrical and Computer Engineering*, vol. 10, no. 6, pp. 6423–6434, 2020.

[36] M. M. Hamdi, L. Audah, S. A. Rashid, and S. Alani, "VANET-based traffic monitoring and incident detection system: A review," *International Journal of Electrical and Computer Engineering*, vol. 11, no. 4, pp. 3193–3200, 2021.

[37] A. Litvinenko, J. Eidaks, and A. Aboltins, 'Usage of signals with a high PAPR level for efficient wireless power transfer," in *Proc. 2018* IEEE *6th Workshop on Advances in Information, Electronic and Electrical Engineering*, 2018.

[38] B. Hasan, S. Alani, and M. A. Saad, 'Secured node detection technique based on artificial neural network for wireless sensor network', *International Journal of Electrical and Computer Engineering*, vol. 11, no. 1, pp. 536–544, 2021.
[39] S. Alani, Z. Zakaria, and H. Lago, "A new energy consumption technique for mobile ad hoc networks," *International Journal of Electrical and Computer Engineering (IJECE)*, vol. 9, no. 5, p. 4147, Oct. 2019.
[40] N. C. E. Chukwu and G. N. Onoh, "Experimental study on the impact of weather conditions on wide code division multiple Access signals IN nigeria," *Engineering, Technology and* Applied *Science Research*, vol. 9, no. 2, pp. 3998–4001, 2019.
[41] S. A. Fathy, M. N. A. Ibrahim, S. S. Elagooz, and H. M. El-Hennawy, "Efficient SLM technique for PAPR reduction in UFMC systems," in *Proc. National Radio Science Conference*, vol. 2019-April, pp. 118–125, 2019.
[42] P. Rani, S. Baghla, and H. Monga, "An improved papr reduction technique for universal filter multi-carrier modulation," *Acta Electrotechnica et Informatica*, vol. 18, no. 1, pp. 41–46, 2018.
[43] P. Rani, S. Baghla, and H. Monga, "Hybrid papr reduction scheme for universal filter multi-carrier modulation in next generation wireless systems," *Advances in Systems Science and Applications*, vol. 17, no. 4, pp. 22–33, 2017.
[44] T. Deepa and R. Kumar, "Performance evaluation of a low complexity row-column transform approach for SLM based ofdm transmission system," *Wireless Personal Communications*, vol. 87, no. 4, pp. 1357–1369, 2016.
[45] P. A. Pushkarev, K. W. Ryu, K. Y. Yoo, and Y. W. Park, "A study on the PAR reduction by hybrid algorithm based on the PTS and SLM techniques," *IEEE Vehicular Technology Conference*, vol. 57, no. 2, pp. 1263–1267, 2003.
[46] N. Carson and T. A. Gulliver, 'Papr reduction of OFDM using selected mapping, modified RA codes and clipping," *IEEE Vehicular Technology Conference*, vol. 56, no. 2, pp. 1070–1073, 2002.
[47] K. Singh, M. R. Bharti, and S. Jamwal, "A modified papr reduction scheme based on SLM and PTS techniques," in *Proc. 2012 IEEE International Conference on Signal Processing, Computing and Control, ISPCC 2012*, 2012.
[48] H. Wang, 'A hybrid papr reduction method based on SLM and multi-data block PTS for FBMC/OQAM systems," *Information (Switzerland)*, vol. 9, no. 10, 2018.
[49] H. Tiwari, R. Roshan, and R. K. Singh, 'Papr reduction in MIMO-OFDM using combined methodology of selected mapping (SLM) and partial transmit sequence (PTS)," in *Proc. 9th International Conference on Industrial and Information Systems*, 2015.
[50] J. Merin Joshiba, D. Judson, and A. A. Raj, "5G modulation techniques — A systematic literature survey," pp. 351–372, 2022.
[51] X. Wang, L. Mei, Z. Wang, and X. Sha, 'Enhanced clipping and filtering with wfrft for papr reduction in OFDM systems," *IEEE Wireless Communications and Networking Conference*, vol. 2019-April, 2019.
[52] S. X. Zhang, J. Zhou, H. B. Zhu, and Q. Zhu, "Cubic metric improvement of aggregated carriers for downlink transmission in LTE-advanced," *Journal of China Universities of Posts and Telecommunications*, vol. 18, no. 1, 2011.
[53] W. Min and Q. Zhengding, "Power de-rating reduction for DFT-S-OFDM system," *IET Conference Publications*, no. 525, p. 234, 2006.
[54] 3GPP, "Technical specification group radio access network; Physical layer aspects for evolved universal terrestrial radio access (UTRA)," *Release*, pp. 1–132, 2006.
[55] X. Yang, X. Zhu, Z. Zeng, and G. Guo, "Analysis of power de-rating represented by maximum power reduction and cubic metric in LTE uplink transmission," in *Proc. 2010 6th* International *Conference on Wireless Communications, Networking and Mobile Computing* , 2010.
[56] H. Emami and A. A. Sharifi, "An improved backtracking search optimization algorithm for cubic metric reduction of OFDM signals," *ICT Express*, vol. 6, no. 3, pp. 258–261, 2020.
[57] T. Assaf, A. J. Al-Dweik, M. S. E. Moursi, H. Zeineldin, and M. Al-Jarrah, "Exact bit error-rate analysis of two-user noma using qam with arbitrary modulation orders," *IEEE Communications Letters*, vol. 24, no. 12, pp. 2705–2709, 2020.
[58] A. Mohammed, T. Ismail, A. Nassar, and H. Mostafa, "A novel companding technique to reduce high peak to average power ratio in OFDM systems," *IEEE Access*, vol. 9, pp. 35217–35228, 2021.
[59] J. Yli-Kaakinen *et al.*, 'Frequency-domain signal processing for spectrally-enhanced CP-OFDM waveforms in 5G new radio," *IEEE Transactions on Wireless Communications*, vol. 20, no. 10, pp. 6867–6883, 2021.
[60] K. Satyavathi and B. Rama Rao, 'Modified phase sequence in hybrid pts scheme for papr reduction in OFDM systems," *Lecture Notes in Networks and Systems*, vol. 33, pp. 327–333, 2019.
[61] N. A. Mohammed, M. M. Elnabawy, and A. A. M. Khalaf, "Papr reduction using a combination between precoding andnon-linear companding techniques foraco-ofdm-based vlc systems," *Opto-Electronics Review*, vol. 29, no. 2, pp. 59–70, 2021.
[62] V. N. Sonawane and S. V. Khobragade, "Comparative analysis between a- law and μ -law companding technique for papr reduction in OFDM," *International Journal of Advanced Research in Computer and Communication Engineering*, vol. 2, no. 5, pp. 2210–2214, 2013.
[63] M. I. Youssef, I. F. Tarrad, and M. Mounir, "Performance evaluation of hybrid ACE-PTS PAPR reduction techniques," in *Proc. 2016 11th International Conference on Computer Engineering and Systems*, pp. 407–413, 2017.